Journal of
NANOSTRUCTURES
JNS
NANOSTRUCTURES
JNS.kashanu.ac.ir

Sono-chemical Synthesis Fe_3O_4-$Mg(OH)_2$ Nanocomposite and Its Photo-catalyst Investigation in Methyl Orange Degradation

G. Nabiyouni *[,a], D. Ghanbari [b], S. Karimzadeh [c] , B. Samani Ghalehtaki [c]

[a] *Department of Physics, Faculty of Science, Arak University, Arak 38156-88349, Iran*

[b] *Young Researchers and Elite Club, Arak Branch, Islamic Azad University, Arak, Iran*

[c] *Institute of Nano Science and Nano Technology, University of Kashan, Kashan, P.O. Box 87317-51167, Iran*

Article history:
Received 11/10/2014
Accepted 13/11/2014
Published online 21/12/2014

Keywords:
Sono-chemical
Fe_3O_4-$Mg(OH)_2$
Nanocomposites

**Corresponding author:*
E-mail address:.
G-nabiyouni@araku.ac.ir
Phone: +98 86 34173401-5
Fax: +98 86 34173406

Abstract

In this work firstly Fe_3O_4 nanoparticles were synthesized via a sono-chemical method. At the second step magnesium hydroxide shell was synthesized on the magnetite-core under ultrasonic waves. For preparation Fe_3O_4-MgO the product was calcinated at 400 ºC for 2h. Properties of the product were examined by X-ray diffraction pattern (XRD), scanning electron microscope (SEM) and Fourier transform infrared (FT-IR) spectroscopy. Vibrating sample magnetometer (VSM) shows nanoparticles exhibit super-paramagnetic behavior. The photo-catalytic behavior of Fe_3O_4-$Mg(OH)_2$ nanocomposite was evaluated using the degradation of a methyl orange (MeO) aqueous solution under ultraviolet (UV) light irradiation. The results show that Fe_3O_4-$Mg(OH)_2$ nanocomposites have applicable magnetic and photo-catalytic performance.

1. Introduction

Fe_3O_4 has exhibited unique electric and magnetic properties based on the transfer of electrons between Fe^{3+} and Fe^{2+} in the octahedral sites. For their low toxicity, good biocompatibility and tunable magnetic properties, magnetite have received considerable attention in various areas such as catalysis, magnetic refrigeration systems, drug delivery and turgeting, heat transfer applications, cancer therapy, enzyme immobilization and magnetic cell separation [1].

Various methods to eliminate pollutants compounds from wastewater have been reported in the literature; among them, the

advanced oxidation processes, in which the photo-degradation processes are included. These processes consist in the decomposition of organic molecules interacting with both, an UV or visible light as well as the interaction with a photo-catalyst material, in order to get CO_2 and H_2O as final products [2]. Several semiconductor materials have been reported in the literatureas such as TiO_2 (effective and most frequently mentioned) ZrO_2, WO_3, ZnO, ZnS, SnO_2, Fe_2O_3, as well as large number of binary, ternary and quaternary mixed oxides.

There is an increasing interest in magnetic ferrite nanoparticles because of their broad applications in several technological fields including permanent magnets, magnetic fluids, drug delivery, microwave devices, and high density information storage [3–5]. Ferrite has been widely studied because it possesses excellent chemical stability and suitable mechanical hardness. In addition to the precise control on the composition and structure of Fe_3O_4 different chemical and physical synthesis methods, such as precipitation, sol-gel, hydrothermal are used to produce magnetite. Among the reported methods, the sonochemical method is an efficient way to production of ultrafine and mono-dispersed magnetite powder [6-10].

Sonochemical method operated under ambient conditions. Ultrasonic waves propagate through the solution causing alternating high and low pressure in the liquid media. Ultrasonic irradiation caused cavitation in a liquid medium where the formation, growth and implosive collapse of bubbles occurred. The collapse of bubbles with short lifetimes produces intense local heating and high pressure. These localized hot spots can generate a temperature of around 5000 °C and a pressure of over 1800 kPa and can drive many chemical reactions [11-16].

One of the most commonly used mineral flame retardants is magnesium hydroxide. As the temperature raises magnesium hydroxide decomposes endothermically (about 330°C with an endothermic of 1.356 kJ/g) and absorbs energy. A variety of synthesis strategies for metal hydroxides nanostructure materials have been described. Sonochemical method as a simple, effective and novel route has been developed to prepare nanostructures.

In the present work, Fe_3O_4 nanoparticles Fe_3O_4-$Mg(OH)_2$ and Fe_3O_4-MgO nanocomposites were synthesized by a surfactant-free sonochemical method without using inert atmosphere. The obtained samples were characterized by scanning electron microscopy and X-ray diffraction pattern. The magnetic properties were investigated using a vibrating sample magnetometer. Magnetic photo-catalysts have gained much attention because those can easily be seperated from polluted waters by applying a simple magnetic field.

2. Experimental

2.1. Materials and Instruments

$Mg(NO_3)_2$ $6H_2O$, $FeCl_2$ $4H_2O$, and NH_3 were purchased from Merck Company. All of the chemicals were used as received without further purifications. XRD patterns were recorded by a Philips, X-ray diffracttometer using Ni-filtered Cu K_α radiation. For SEM images the samples were coated by a very thin layer of Au to make the sample surface conductor and prevent charge accumulation, and obtaining a better contrast. Room temperature magnetic properties

were investigated using a vibrating sample magnetometer (VSM, made by Meghnatis Daghigh Kavir Company) in an applied magnetic field sweeping between ±10000 Oe.

A multiwave ultrasonic generator (Sonicator 3000; Bandeline, MS 73, Germany), equipped with a converter/transducer and titanium oscillator (horn), 1.25×10^{-2} m in diameter, surface area of ultrasound irradiating face: 1.23×10^{-4} m^2, operating at 20 kHz, was used for the ultrasonic irradiation and the horn was operated at 50% amplitude. All ultrasonication experiments were carried out at ultrasonic power between 84–125 mW measured by calorimeter.

2.2. Synthesis of nanoparticles and nanocomposites

1 g of $FeCl_2$ $4H_2O$ is dissolved in 100 ml of distilled water. 15 ml of NH_3 solution (5M) is slowly added to the solution under ultrasonic irradiation 75 W and 20min. A black precipitate is obtained confirming the synthesis of Fe_3O_4. The precipitate of Fe_3O_4 is then centrifuged and rinsed with distilled water, followed by being left in an atmosphere environment to dry. Fig.1a shows the schematic diagram for experimental setup used in this sono-chemical method.

In step 2 nanoparticles were dispersed in water solution and $Mg(NO_3)_2$ $6H_2O$ was dissolved in the solution simultaneously. 10 ml of ammonia was added to solution under sonication (75 W, 20 min, Fig 1b). The precipitate of Fe_3O_4-$Mg(OH)_2$ is then centrifuged and rinsed with distilled water. For preparation Fe_3O_4-MgO , the sample was calcinated at 400 ºC for 2h.

3. Results and discussion

The XRD pattern of Fe_3O_4 nanoparticles is shown in Fig. 2. The pattern of as-prepared Fe_3O_4 nanoparticles is indexed as a pure cubic phase which is very close to the literature values (JCPDS No. 75-0449). Space group of magnetite is Fd3m. The narrow sharp peaks indicate that the Fe_3O_4 nanoparticles are well crystallized.

The crystallite size measurements were also carried out using the Scherrer equation,

$$D_c=K\lambda/\beta Cos\theta$$

Where β is the width of the observed diffraction peak at its half maximum intensity (FWHM), K is the shape factor, which takes a value of about 0.9, and λ is the X-ray wavelength (CuK_α radiation, equals to 0.154 nm). The estimated crystallite size was about 8 nm.

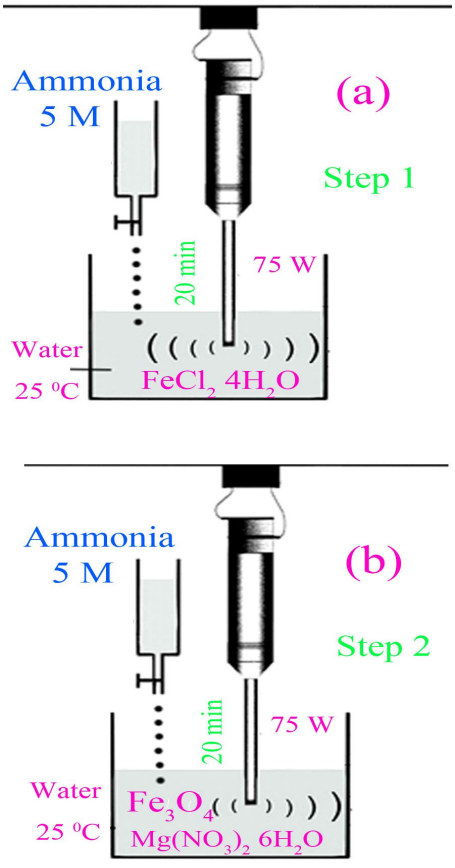

Fig. 1. Schematic of sono-chemical preparation of (a) Fe_3O_4 nanoparticles (b) Fe_3O_4-$Mg(OH)_2$ nanocomposite.

The XRD pattern of $Mg(OH)_2$ nanoparticles is illustrated in Fig. 3. The pattern of $Mg(OH)_2$ nanoparticles confirms a pure hexagonal phase which is very close to the literature values (JCPDS No. 84-2164). The sharp peaks approve high crystalinity of the magnesium hydroxide nanoparticles.

The XRD pattern of Fe_3O_4-$Mg(OH)_2$ nanocomposite is shown in Fig. 4. The pattern of Fe_3O_4-$Mg(OH)_2$ nanocomposite shows two phases of magnetite and magnesium hydroxide with JCPDS numbers of 84-2164 and 75-0449 simultaneously.

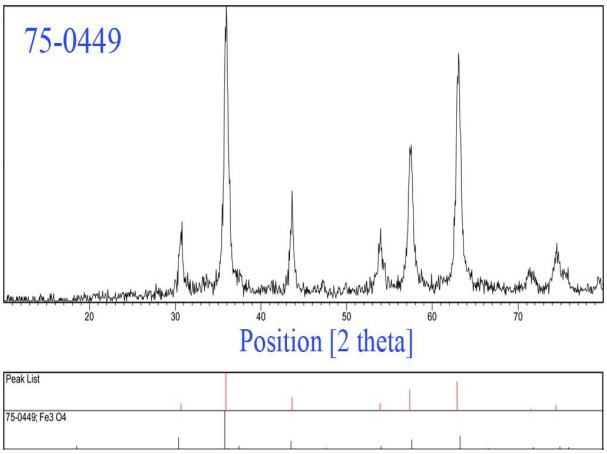

Fig. 2. XRD pattern of the Fe_3O_4 nanoparticles

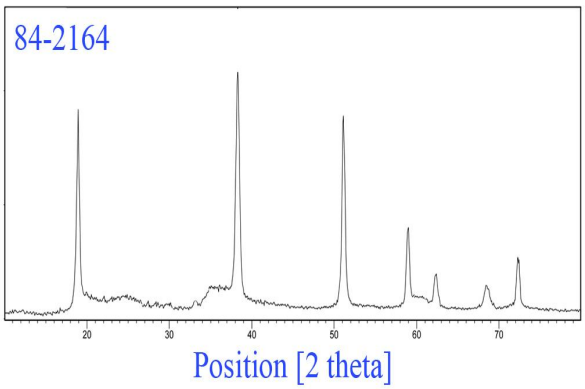

Fig. 3. XRD pattern of the $Mg(OH)_2$ nanoparticles

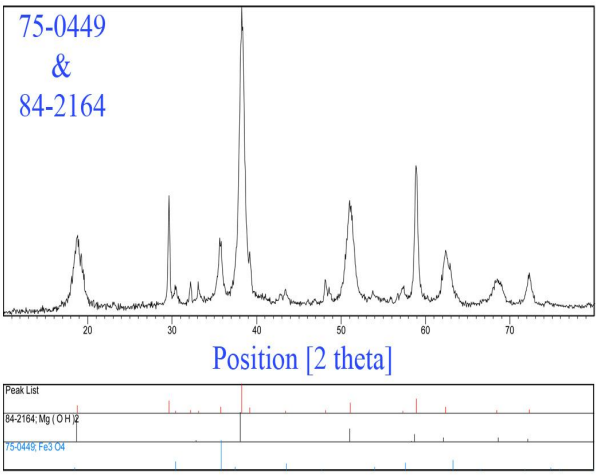

Fig. 4. XRD pattern of the Fe_3O_4-$Mg(OH)_2$ nanocomposite.

Fig. 5 illustrates SEM images of synthesized Fe_3O_4 nanoparticles that confirm average diameter size of product is less than 50 nm.

SEM images of Fe_3O_4-$Mg(OH)_2$ are studied and illustrated in Fig.6. According to images particles with average diameter of 60 nm are obtained. For better investigation of nanocomposite transmission electron microscopy is needed.

The image shows that the sample consists of larger particles compare to pure magnetite nanoparticles.

During the ultrasound cycles, the cavitation bubbles would collapse, forming micro-jets that instantaneously generate intense local heating and high pressure. The micro-jet impact can develop pressures of about 2×10^8 Pa, and a local heating and cooling rate above 10^9 K/s. In fact, cavitation damage is generated by the non-spherical symmetric collapse of a cavitation bubble, either at or near a solid surface. Violent collapse of bubbles in asymmetrical geometries occur in a number of situations of practical interest including cavitation, shock-wave and laser lithotripsy [14,16].

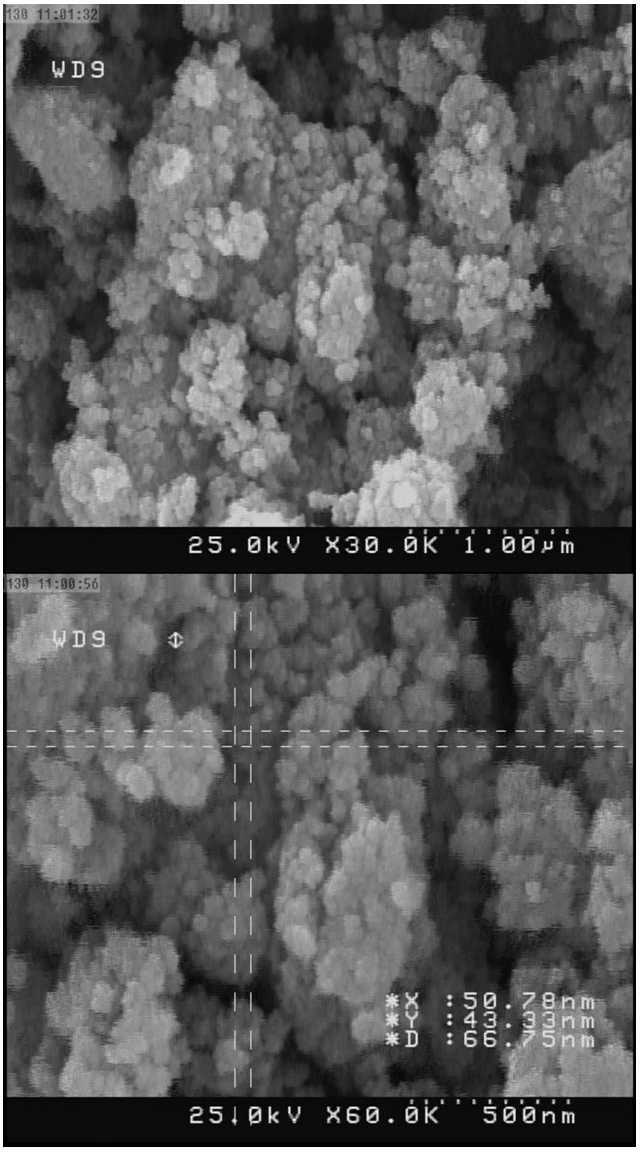

Fig. 5. SEM images of Fe_3O_4 nanoparticles.

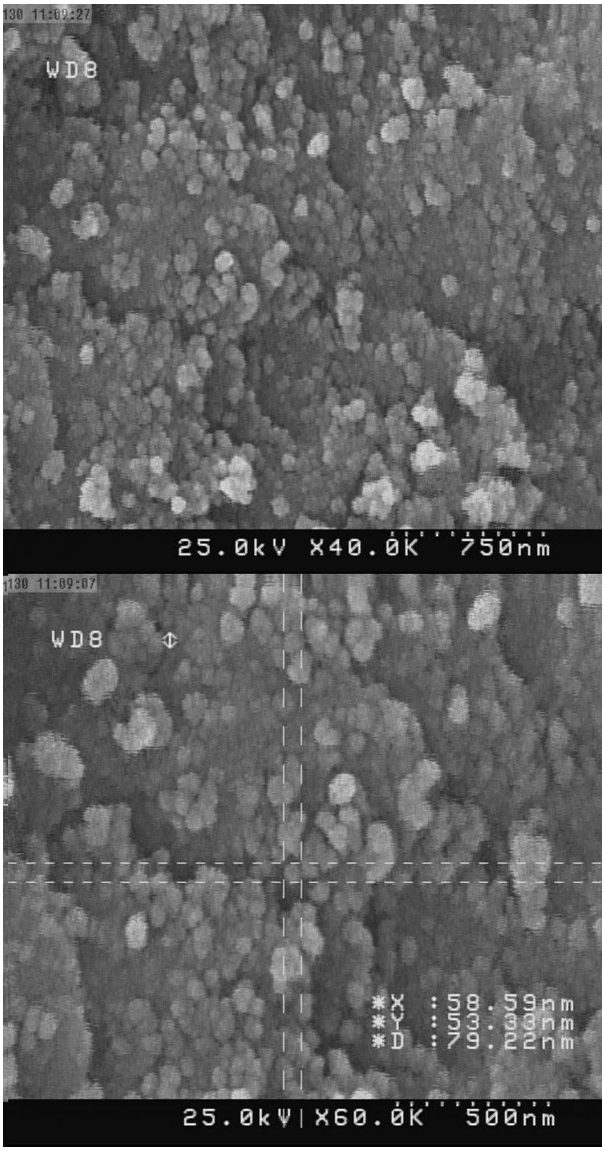

Fig. 6. SEM images of Fe_3O_4-$Mg(OH)_2$ nanocomposite

This method proposes easy manipulation in particle size and so magnetic properties by a simple change in power, time of irradiation, precursor, temperature and solvent.

Fig. 7 illustrates SEM images of Fe_3O_4-MgO nanocomposite that is obtained at 400 ºC and confirms some agglomeration compare to magnetite-magnesium hydroxide. It seems with calcination growth stage is predominant compare to nucleation stage.

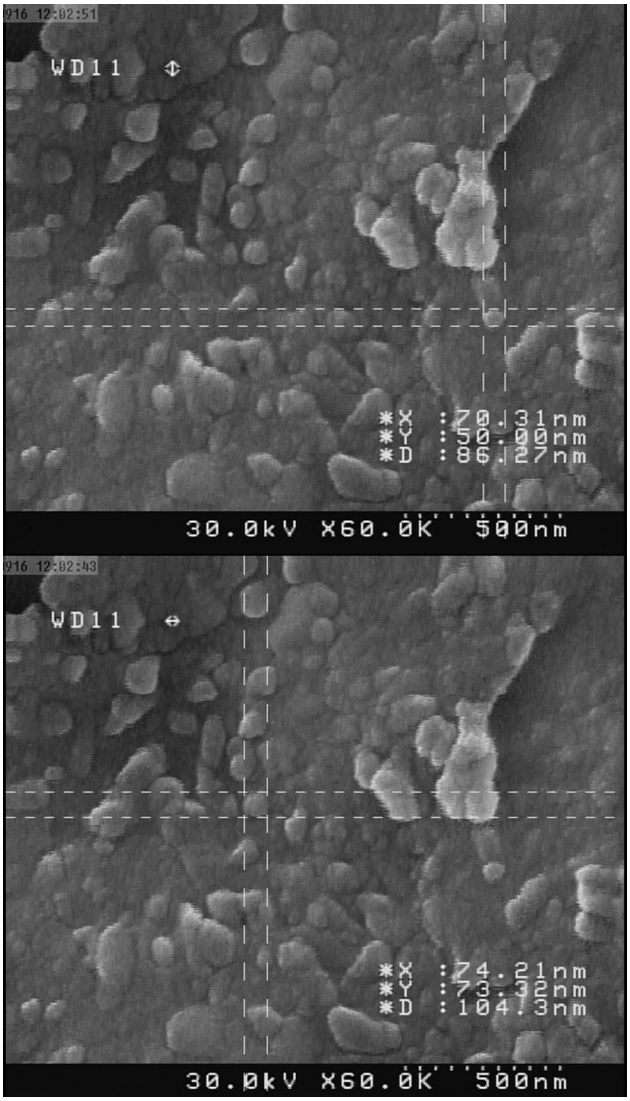

Fig. 7. SEM images of Fe_3O_4-MgO nanocomposite

Room temperature magnetic properties of samples are studied using a VSM device. Hysteresis loop for magnetite nanoparticles is depicted in Fig. 8.

Fe_3O_4 synthesized nanoparticles show super-paramagnetic behavior and have a saturation magnetization of 68 emu/g and very low coercivity.

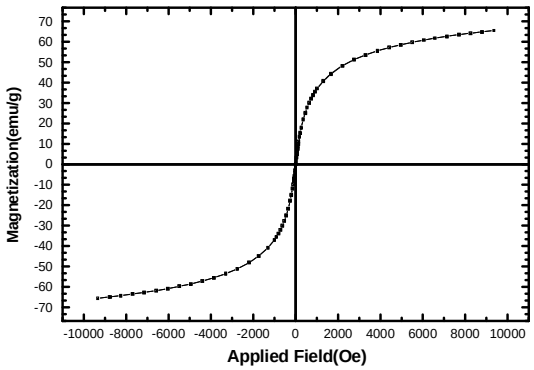

Fig. 8. Hysteresis curve of Fe_3O_4 nanoparticles

Fig. 9 shows magnetization curve of Fe_3O_4–$Mg(OH)_2$ nanocomposites that also exhibits super-paramagnetic behavior with a very low coercivity and a saturation magnetization of 41 emu/g. As expected due to presence of magnesium hydroxide, its magnetization is lower than pure Fe_3O_4 nanoparticles.

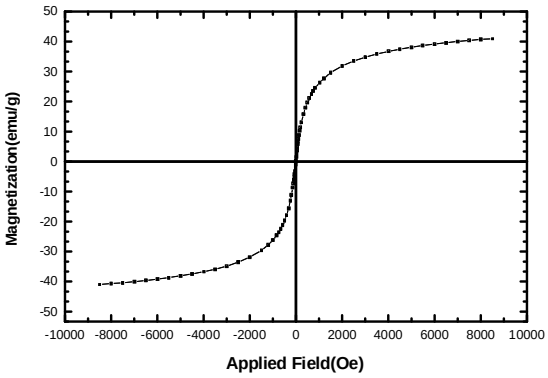

Fig. 9. Magnetization curve of Fe_3O_4-$Mg(OH)_2$ nanocomposite.

Fourier transform infra-red (FT-IR) spectrum of synthesized nanoparticles was recorded in the range of 400–4000 cm^{-1} and result is shown in Fig. 10. Absorption peaks around 420 and 593 cm^{-1} are related to metal-oxygen Mg-O and Fe-O bonds. The spectrum exhibits broad absorption peaks between 3500-3600 cm^{-1},

corresponding to the stretching mode of O-H group of $Mg(OH)_2$ and also hydroxyl group that are adsorbed on the surface of nanoparticles.

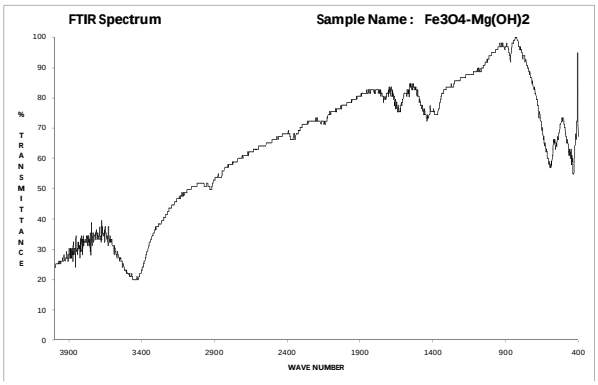

Fig. 10. FT-IR spectrum of Fe_3O_4-$Mg(OH)_2$ nanocomposite.

The photo-catalytic activity of the nanocomposite was evaluated by monitoring the degradation of methyl orange (MeO) in an aqueous solution. 0.1 g of magnetic nanocomposite was dispersed in 10 ml of MeO solution (3ppm). Pure methyl orange and MeO under UV irradiation in the presence of Fe_3O_4-$Mg(OH)_2$ (20, 40 and 60 min) are illustrated in Fig 11a-d respectively.

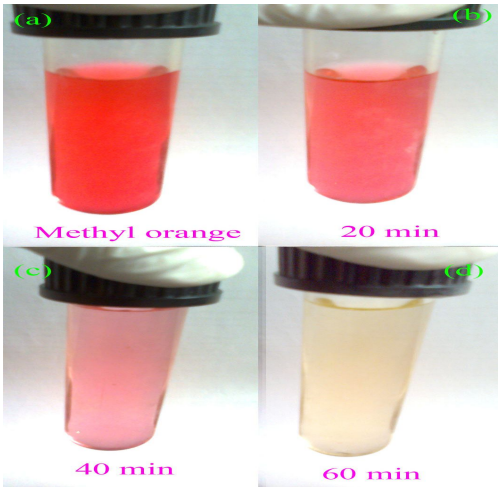

Fig. 11. Effect of Fe_3O_4-$Mg(OH)_2$ under UV irradiation (a) Methyl orange (b) 20 min (c) 40 min (d) 60 min.

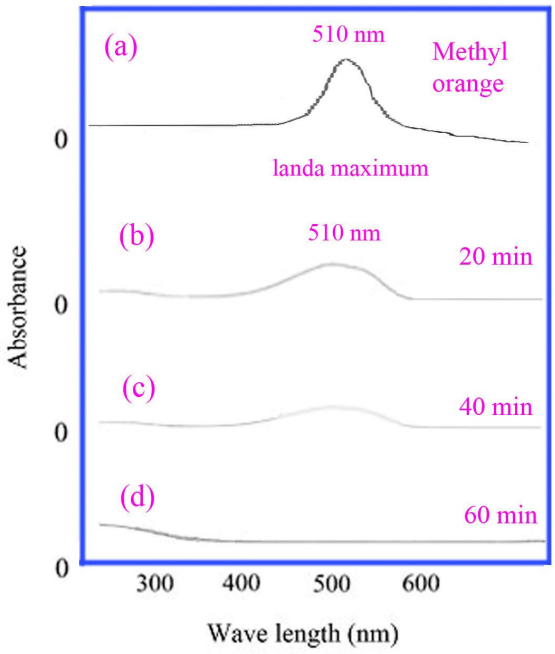

Fig. 12. UV-visible absorption of (a) Methyl orange (b) 20 min (c) 40 min (d) 60 min.

4. Conclusion

Magnetite nanoparticles were synthesized via a sono-chemical method. Then $Mg(OH)_2$ shell was synthesized on the magnetite-core. For synthesis Fe_3O_4-MgO the product was calcinated at 400 ºC for 2h. Vibrating sample magnetometer confirms nanoparticles and nanocomposites exhibit super-paramagnetic behavior. The photocatalytic behavior of Fe_3O_4-$Mg(OH)_2$ nanocomposite was evaluated using the degradation of a methyl orange aqueous solution under UV light irradiation. The results show that Fe_3O_4-$Mg(OH)_2$ nanocomposites are promising materials with suitable performance in photo-catalytic applications.

Acknowledgments

This work has been supported financially by Arak University Research Council (AURC) under the grant number of 93/4656 [5-6-93].

The authors acknowledge AURC for the financial support.

References

[1] D. Ghanbari, M. Salavati-Niasari, M. Ghasemi-Koch, J Indus Eng Chem. 20 (2014) 3970-3974.

[2] F. Tzompantzi, Y. Pina, A. Mantilla, O. Aguilar-Martínez, F. Galindo-Hernandez, Xim Bokhimi, A. Barrera. Catal Today 222 (2014) 49– 55.

[3] H.R. Momenian, M. Salavati-Niasari, D. Ghanbari, B. Pedram, F. Mozaffar, S. Gholamrezaei, J Nano Struc. 4 (2014) 99-104.

[4] F. Zhang, S. Kantake, Y. Kitamoto, M. Abe, IEEE Trans. Magn. 35 (1999) 2751–2753.

[5] Y. Kitamoto, S. Kantake, S. Shirasaki, F. Abe, M. Naoe, J. Appl. Phys. 85 (1999) 4708-4710.

[6] A.E. Berkowitz, W. Schuele, J. Appl. Phys. 30 (1959) 134–135.

[7] G. Nabiyouni, S. Sharifi, D. Ghanbari, M. Salavati-Niasari, J Nano Struc. 4 (2014) 317-323.

[8] K. Maaz, A. Mumtaz, S.K. Hasanain, A. Ceylan, J. Magn. Magn. Mater 308 (2007) 289-295.

[9] X. Chu, D. Jiang, Y. Guo, C. Zheng, Sens. Actuator B. 120 (2006) 177.-181

[10] C.C. Wang, I.H. Chen, C.R. Lin, J. Magn. Magn. Mater. 304 (2006) 451-453.

[11] Y.I. Kim, D. Kim, C.S. Lee, Phys. B 337 (2003) 42-51.

[12] Y. Shi, J. Ding, H. Yin, J. Alloys Compd. 308 (2000) 290-295.

[13] S. Gholamrezaei, M. Salavati-Niasari, D. Ghanbari, J Indus Eng Chem. 20 (2014) 3335-3341.

[14] P. Jamshidi, M. Salavati-Niasari, D. Ghanbari, H.R. Shams, J Clust Sci. 24 (2013) 1151-1162

[15] S. Gholamrezaei, M. Salavati-Niasari, D. Ghanbari, J Indus Eng Chem. 20 (2014) 4000-4007.

[16] H.R. Momenian, S. Gholamrezaei, M. Salavati-Niasari, B. Pedram , F. Mozaffar , D. Ghanbari, J Clust Sci. 24 (2013) 1031-1042.